Spleen voltammetry assesses in real time norepinephrine release elicited by autonomic stimulation

Ibrahim T. Mughrabi[1,¶], Michael Gerber[1,¶], Naveen Jayaprakash[1], Yousef Al-Abed[1], Stavros Zanos[1,*]

[1] Institute of Bioelectronic Medicine, The Feinstein Institutes for Medical Research, Manhasset, NY, USA.

* Corresponding author
E-mail: szanos@northwell.edu

¶ These authors contributed equally to this work

Abstract

Bioelectronic medicine uses neurostimulation devices to modulate the activity of autonomic nerves and restore function in visceral organs. The autonomic, noradrenergic, innervation of the spleen is implicated in the neural control of inflammation; for that reason, the spleen is the target of autonomic stimulation therapies tested in rheumatoid arthritis and other inflammatory diseases. However, there are no real time markers for successful engagement of the spleen by autonomic stimulation. Here, we use fast-scan cyclic voltammetry (FSCV) in the spleen to assess, in real time, the release of norepinephrine (NE) in response to autonomic stimulation in mice. We show that spleen voltammograms demonstrate oxidative current peaks at a voltage of ~0.8 V that is proportional up to a NE blood concentration of 30 to 300nM. The oxidative current increases within seconds in response to electrical splenic nerve stimulation and is blocked by interventions that deplete NE or inhibit NE release. Oxidative current increases in response to electrical vagus nerve stimulation (VNS) and is elicited by efferent, but not afferent, fiber-selective optogenetic VNS. Spleen cyclic voltammetry can potentially provide a real-time physiological marker for dose calibration and monitoring of the anti-inflammatory effectiveness of autonomic stimulation therapies targeting the spleen.

Introduction

The autonomic nervous system (ANS) helps maintain internal homeostasis through a network of neural reflexes. Sensory and motor signaling in autonomic reflexes regulates physiological functions such as respiration, blood pressure, heart rate and digestion[1]. Recently, the autonomic innervation of the spleen through the splenic nerve has been implicated in the neural control of inflammation [1]. It was found that modulation of the activity of the splenic nerve by electrical stimulation inhibits the inflammatory response [2]. Subsequent mechanistic studies revealed that some of these anti-inflammatory effects are initiated by release of norepinephrine (NE) in the spleen upon autonomic nerve stimulation [3]. In response to those observations, a new class of therapies, collectively termed bioelectronic medicine or autonomic neuromodulation therapies, aims at treating chronic inflammatory diseases by modulating the activity of autonomic nerves with neurostimulation devices [4]. Devices for cervical vagus nerve stimulation (VNS) [5], trans-auricular VNS [6, 7], splenic nerve stimulation [2], and ultrasound stimulation of the spleen [8] target the autonomic innervation of the spleen to suppress inflammation in patients with rheumatoid arthritis and other inflammatory diseases [9].

During the clinical programing of bioelectronic therapies, parameters of neurostimulation need to be calibrated to maximize anti-inflammatory efficacy and minimize unwanted effects of stimulation [4]. For example, excessive stimulation of the cervical vagus, that also innervates the larynx and the heart, leads to coughing or heart rate reduction [10, 11]. To optimize and calibrate stimulation in individual subjects, direct, organ-specific physiological responses need to be measured to determine whether and to what extent the autonomic innervation of an organ is engaged. Whereas such responses are readily available for organs like the heart, lungs and gut [12, 13], no such physiological marker exists for the engagement of the autonomic innervation of the spleen. As a result, stimulation parameters in anti-inflammatory bioelectronic therapies are determined empirically, are difficult to be personalized and are potentially sub-optimal. A real time method for assessing the response of the spleen to autonomic stimulation could contribute to safer and more effective anti-inflammatory bioelectronic therapies.

In this study, we developed a method to assess real time release of NE in the mouse spleen in response to autonomic stimulation using FSCV, an electrochemical method used to measure

neurotransmitter release in living tissue. We find that voltammetry in the spleen produces a signal that tracks in vivo concentration of NE and responds to electric and optogenetic autonomic stimulation. We also find that the amplitude of the stimulation-elicited voltammetry signal predicts the degree of suppression of TNF release in acute inflammation. Our findings indicate that voltammetry may be a feasible approach to assess in real time release of NE in the spleen during autonomic stimulation and potentially assist in the clinical programing of anti-inflammatory bioelectronic therapies.

Methods

Animals

Male and female C57BL/6 mice, ages 8-16 weeks, were purchased from Charles River Laboratories (Wilmington, MA). ChAT-IRES-Cre (#006410), Vglut2-IRES-Cre (#016963), and Ai32 ChR2-eYFP (#024109) mice were purchased from The Jackson Laboratory (Bar Harbor, ME) and crossed to produce ChAT-ChR2-eYFP and Vglut2-ChR2-eYFP mice used for optogenetic experiments. Animals were housed using a 12-hour light/dark cycle with ad libitum access to food and water. All animal procedures were approved by the Institutional Animal Care and Use Committee (IACUC) of the Feinstein Institutes for Medical Research, NY and complied with relevant NIH policies and guidelines.

Surgical procedures

Following isoflurane anesthesia, induced at 4% and maintained at 1.5%, a 2-cm midline abdominal incision was made through the linea alba to just above the xyphoid process. The spleen was gently exposed by retracting the stomach and gut to the right while blunt dissecting the gastrosplenic ligament. The lower branch of the splenic neurovascular bundle was identified and gently dissected from surrounding fat. The spleen was then lifted out of the abdominal cavity and supported with cotton tips. A 34-μm diameter carbon fiber microelectrode (CFM; Pinnacle) and an Ag/AgCl reference electrode were mounted on a stereotaxic manipulator and inserted into the exposed spleen. The voltammetry electrodes were advanced ~0.5 mm into the diaphragmatic surface of the spleen opposite to the inferior branch of the splenic neurovascular bundle supplying the lower half of the spleen (Fig 1a). In some experiments, the splenic neurovascular bundle was placed into a bipolar micro-cuff electrode to deliver electrical stimulation to the splenic nerve, which runs along the splenic artery. To isolate the left cervical vagus nerve, a 1-cm midline incision was made in the anterior neck and the salivary glands were retracted laterally along with the sternocleidomastoid muscle. The vagus nerve was then identified within the carotid sheath and dissected away from connective tissue then gently placed on a bipolar micro-cuff electrode for electrical stimulation or a custom-made optical cuff for optogenetic stimulation.

Fast-scan cyclic voltammetry

A two-electrode commercial system (Pinnacle Technology Inc, Lawrence, KS) was used to perform FSCV using a triangular waveform scanning from -0.4 to 1.3 to -0.4 V at 400 V/sec with a cycling frequency of 10 Hz and -0.4 V holding potential between cycles. Electrochemical data was acquired using the continuous scanning mode with triggers introduced after 10 sec of background current recording. In vitro control experiments were performed in PBS and blood using the same FSCV parameters. Blood from multiple animals was collected by cardiac puncture using a heparin-flushed syringe then pooled together before aliquoting into a 96-well plate. Freshly made NE in PBS solution was added to each well to achieve a final concentration of 0, 0.1, 1, and 10 μM. After recording background current from the vehicle treated well, NE was probed in the remaining wells starting with the lowest concentration.

Intravascular infusions

To establish an intravascular (IV) line, the right external jugular vein was isolated and ligated rostrally while blocking blood flow with a loose suture caudally to prevent bleeding. A small incision was then made between the two sutures and a 1-French catheter (Instech Labs, Plymouth Meeting, PA) was advanced into the vessel followed by a 50 μl saline bolus to confirm patency. In some experiments, 100uL norepinephrine (NE) bitartrate boluses were administered sequentially at escalating doses (10ug/mL, 2ug/mL, 0.2ug/mL) 10 minutes apart. The final concentration of circulating NE after each dose was estimated for an average mouse weight of 25 g based on a volume of distribution of 2mL estimated to be total blood volume in a mouse [14]. To induce autonomic reflexes, IV esmolol boluses (10-40 mg/kg) were administered ~25 minutes apart. All IV injections were prepared in saline and administered as 100 μl boluses over 10 seconds.

Nerve stimulation

Electrical stimulation was delivered using commercial bipolar micro-cuff electrodes (CorTec, Freiburg, Germany) or custom-made flexible electrodes (Flex) connected to a stimulus generator (MCS, info). Stimulus trains consisted of bi-phasic charge-balanced square pulses of 10 sec duration, 500 μs pulse width (PW), and 10 Hz frequency at varying intensities. In some experiments, the splenic nerve was blocked by applying a piece of gauze saturated with 2% lidocaine on the splenic neurovascular bundle for 10 min. In cervical vagotomy experiments, the vagus nerve was stabilized on the micro-cuff electrode by applying a drop of 2-component silicone (Kwik-Sil, World Precision instruments, Sarasota, FL) then sectioned either caudal or rostral to the cuff. For optogenetic stimulation experiments, a custom-made optical cuff, consisting of a blue LED light (XLAMP XQ-E, Cree LED, Durham, NC) integrated into a molded silicone cuff, was connected to a stimulus generator (MCS) operating in voltage mode. Optical stimulation was delivered using 10-sec stimulus trains of 10 ms PW and 30 Hz frequency while varying intensity by changing the voltage driving the LED. During vagus stimulation experiments, animals were instrumented with ECG leads and nasal airflow temperature sensors to monitor heart rate and breathing rate responses.

Norepinephrine depletion

Reserpine (info, in DMSO) was diluted in saline and administered to animals by i.p. injection (5 mg/kg). 18-24 hours post-injection, NE elicited by sp-stm was probed using voltammetry in the spleen as described.

Data analysis and statistics

Voltammograms were first background-subtracted and smoothed with a moving average filter. The NE signal was quantified by computing the integral of oxidation current (i^o) over time to generate oxidative charge (Q^o) for each stimulation experiment. This method was chosen because integration of multiple voltammograms was more robust than choosing the highest peak attained after stimulation. An

algorithm was created to determine integration boundaries with the following steps: 1) determine whether NE signal exists, and if so define rough boundaries in the time domain, 2) determine oxidation potential (E^o) of NE within that stimulus experiment, 3) calculate i^o for each voltammogram within rough boundaries and define new boundaries based on the maximum signal, 4) integrate over new boundaries to find Q^o.

First, characterization of the signal was performed by using in vivo NE infusions as positive controls. A characteristic voltammogram was defined by averaging the resulting voltammogram from 5 separate NE infusions from separate animals. In each subsequent experiment, signal detection was done by cross correlating the time-ordered voltammograms with the characteristic voltammogram. This cross correlation was used to determine the upper and lower bounds of the signal under the assumption that a stimulus would increase norepinephrine above baseline levels and then decrease back to baseline over time; the lower bound was defined as the start of the stimulus and the upper bound was defined as the first zero of the cross correlation after the maximum peak. If a valid upper bound defined by these criteria could not be found, or if no stimulus occurred in the experiment, the oxidation charge was considered zero. Between these boundaries, the voltammograms are averaged, filtered and MATLAB's peak detection algorithm is used to determine E^o, as shown in figure 1b. i^o is then defined at E^o as the length of the line drawn between the voltammogram and the tangent between troughs on either side of the peak as shown in figure 1b. A new upper bound is then defined where i^o decreases to 10% of its maximum after the peak. These new boundaries between the start of the stimulus and the point where the signal decreases to 10% of its maximum are used to integrate i^o to compute Q^o.

In experiments where animals served as their own controls (i.e lidocaine nerve suppression, vagotomy, etc), a stimulus that generated the highest signal value was chosen to compute E^o and that was applied to all other stimuli from that same animal, including post treatment where the signal may have disappeared. In reserpine experiments, where animals were not their own controls, an average E^o was computed for all sham subjects and applied to the voltammograms from both groups. Notably, integration boundary calculations were still applied as previously described for each stimulus independently.

Student's two-tailed t-test was used to determine significance in comparisons between two groups (i.e lidocaine, reserpine, vgx, etc.). MATLAB's model fitting package was used for linear regression analysis and computation of r^2. P values less than 0.05 were considered significant. All calculations were done in MATLAB.

Results

Peak oxidation current in spleen voltammogram represents norepinephrine concentration transients in blood

We performed FSCV in vitro to determine the oxidation potential of NE in PBS and blood using biologically relevant NE concentrations. We found that in PBS, NE waveform shape and oxidation potential is 0.6V. In blood, the oxidation potential is 0.71V; the waveform of the voltammogram is similar to that of PBS but involves broader current changes over the voltage sweep (Fig 1b). Furthermore, oxidation potential in blood varies with increasing concentration; 0.71V at 1uM, 0.81V at 10uM and 0.89V at 100uM (Fig 1c).

We next performed FSCV in the mouse spleen during systemic NE injections, to determine whether oxidation current in the spleen voltammogram tracks transient changes in NE concentration in blood. The spleen is a blood-filled organ with a relatively thick connective tissue capsule. Using a larger CFM (34 μm) and pin-tip reference electrode allowed penetration of the capsule and established a stable interface with no bleeding (Fig 1a). NE was injected through the jugular vein at doses estimated to produce peak NE concentration comparable to what has been reported in autonomic stimulation studies (30-60 nM). During NE infusion, voltammograms from the spleen show a similar oxidation phase compared to in vitro experiments, however the reduction phase appears to be inverted (Fig. 1b). In vivo oxidation potential is higher than that measured in vitro (Fig. 1c). The amplitude of the oxidation current increases with increasing NE concentration and is only faintly visible at the lowest concentration (Fig.1d). Since the signal reached consistently non-zero values at 300 nM, the NE detection level of this method was estimated to lie between 30 nM and 300 nM (Fig. 1e).

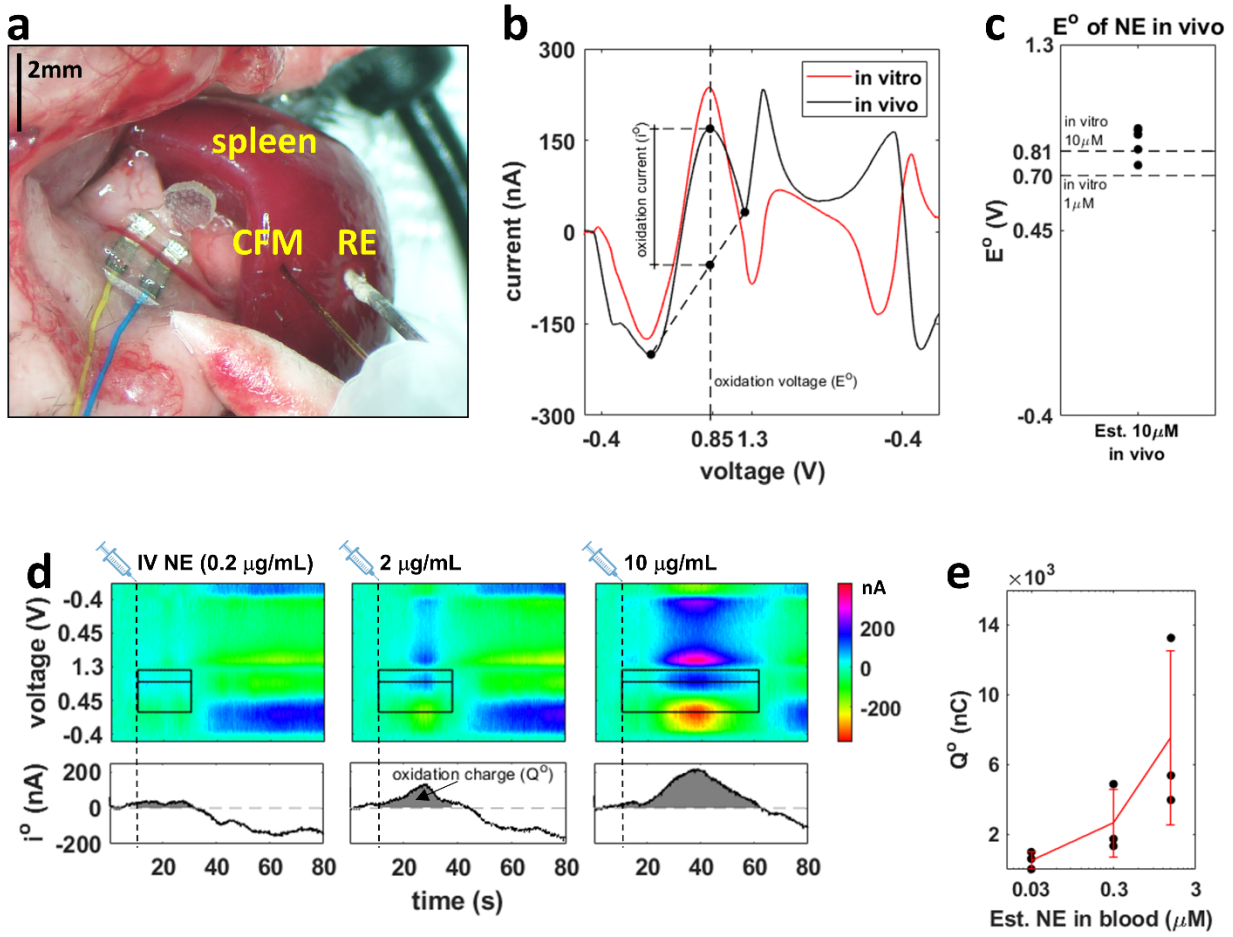

Figure 1. NE Peak oxidation current in spleen voltammograms tracks NE concentration in blood. (a) Placement of electrodes for FSCV in the spleen. A carbon fiber microelectrode (CFM) and reference electrode (RE) are inserted into the spleen. The splenic bundle is cuffed with a bipolar stimulation electrode. (b) NE voltammogram representing peak redox currents recorded during voltage sweep (-0.4 to 1.3 to -0.4) in vitro (heparinized blood, 10 uM NE) and in vivo (live spleen, 1.5 uM NE). (c) NE peak oxidation current potentials from 4 animals recorded in vivo after IV injection of 10 mg/mL NE. (d) Representative voltammograms during NE IV infusion. *Top panels*: Current amplitude (color scale) at different values of sweeping voltage (ordinate) at different times relative to NE injection (abscissa). The outer black box defines the voltage and time boundaries of the peak oxidation current signal (outer boundaries); horizontal line inside box marks the oxidation potential for NE. The dashed vertical line denotes time of drug administration. *Bottom Panels*: oxidation current calculated as shown in figure 1B over the period of sweeping. The grey-shaded area under the curve represents the total oxidation charge (Q^o) generated during the time boundary indicated in the top panels. (e) Oxidation charge at multiple NE concentrations measured in 3 animals for each NE concentration.

Spleen voltammogram represents NE release in response to electrical stimulation of the splenic nerve

Electrical stimulation of the splenic neurovascular bundle (SpNV) is thought to elicit release of NE in the spleen [2]. When delivering stimulation to the SpNV using a cuff electrode (Fig. 1a), oxidation current rises and then settles back to baseline (Fig. 2a). The shape of the voltammograms is similar to that recorded during infusion experiments and is dependent on intensity and duration of the stimulus (Fig. 2a). The oxidation charge is strongly correlated with stimulus intensity (r^2=0.7; Fig. 2b). To verify that the voltammetry signal elicited from SpNV stimulation is at least partly mediated by release of NE, we performed voltammetry in response to SpNV stimulation in animals treated with reserpine to deplete monoamines [15] In reserpine-treated animals the characteristic signal is absent; in contrast, the voltammetry signal is evoked in sham-treated animals (Fig. 2c). To verify the source of released NE, SpNV stimulation was delivered before and after application of lidocaine, a local anesthetic blocking nerve depolarization, directly on the SpNV. The voltammetry signal after lidocaine application is significantly smaller compared to the signal pre-lidocaine (Fig. 2d).

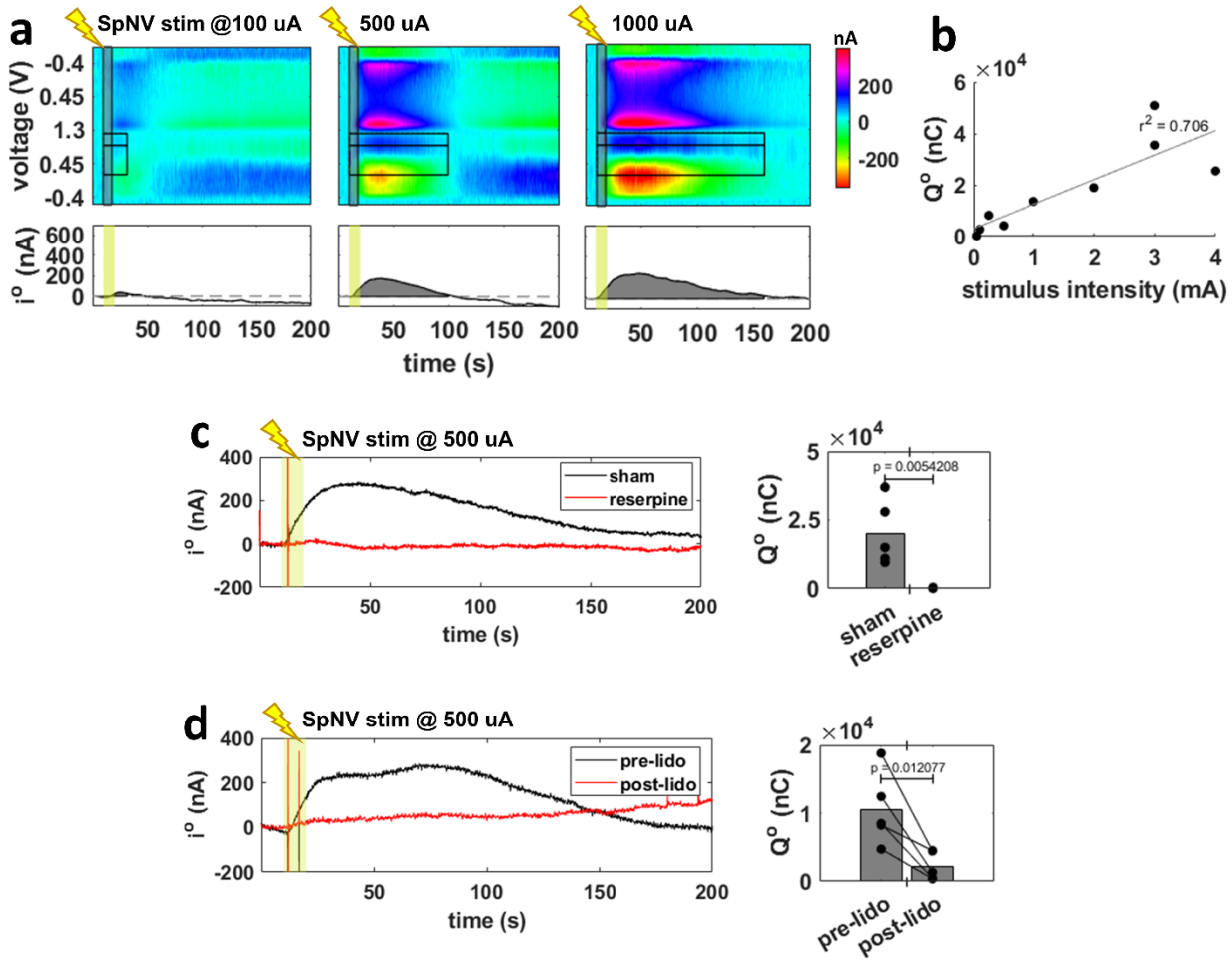

Figure 2. Stimulation of the splenic neurovascular bundle (SpNV) elicits a NE signal in the spleen voltammogram. (a) Representative voltammograms elicited by stimulation of the SpNV. *Top and bottom panels* similar to those of Figure 1d. Dashed vertical line indicates the time of SpNV stimulation. (b) Oxidation charge vs. intensity of SpNV stimulation (one representative of 3 animals). (c) *Left panel:* Examples of time course of NE peak oxidation current in response to SpNV stimulation, in reserpine- and sham-treated mice. *Right panel:* Charge (Q^O) generated by sp-stm in reserpine-treated compared with vehicle-treated animals (n = 4 in each group). (d) *Left panel:* Representative current plot recorded over the period of sweeping in an animal receiving sp-stm before compared with after the application of lidocaine to SpNV *Right panel:* Charge (Q^O) generated by sp-stm in animals before compared with after SpN blockade with lidocaine (n = 4).

Spleen voltammogram represents NE release in response to vagus nerve stimulation

Vagus nerve stimulation (VNS) elicits norepinephrine release in the spleen via the efferent arc of the inflammatory reflex [3]. When delivering VNS via a cuff electrode placed on the cervical vagus, a voltammogram similar to that observed after NE injection is elicited (Fig. 3a); notably, the voltammogram signal in response to VNS has lower amplitude and shorter duration compared to that elicited by SpNV stimulation (Fig. 3a). NE oxidation charge is strongly correlated with VNS intensity (r^2=0.87) (Fig. 3b). To determine the contribution of activation of afferent (sensory) and efferent (motor) vagus fibers to the observed voltammetry signal, VNS was delivered before and after caudal or rostral surgical vagotomies. In response to cervical VNS, activation of afferent fibers elicits changes in breathing and of efferent fibers in heart rate [16]. When VNS is delivered after caudal vagotomy, heart rate response disappears, breathing response is maintained, and the NE signal in the voltammogram is diminished (Fig. 3c). When VNS is delivered after rostral vagotomy, heart rate response is intact, breathing response disappears, and the NE signal in the voltammogram is not affected (Fig. 3d). Similarly, selective activation of efferent vagus fibers by optogenetic VNS in ChAT-ChR mice elicits the NE signal in the voltammogram, whereas optogenetic VNS in Vlut2-ChR mice does not elicit a NE signal. (Fig. 3e). Notably, a rapid decrease heart rate after injection of esmolol, a cardio-selective beta-adrenoceptor blocking agent, elicits a NE signal in the voltammogram.

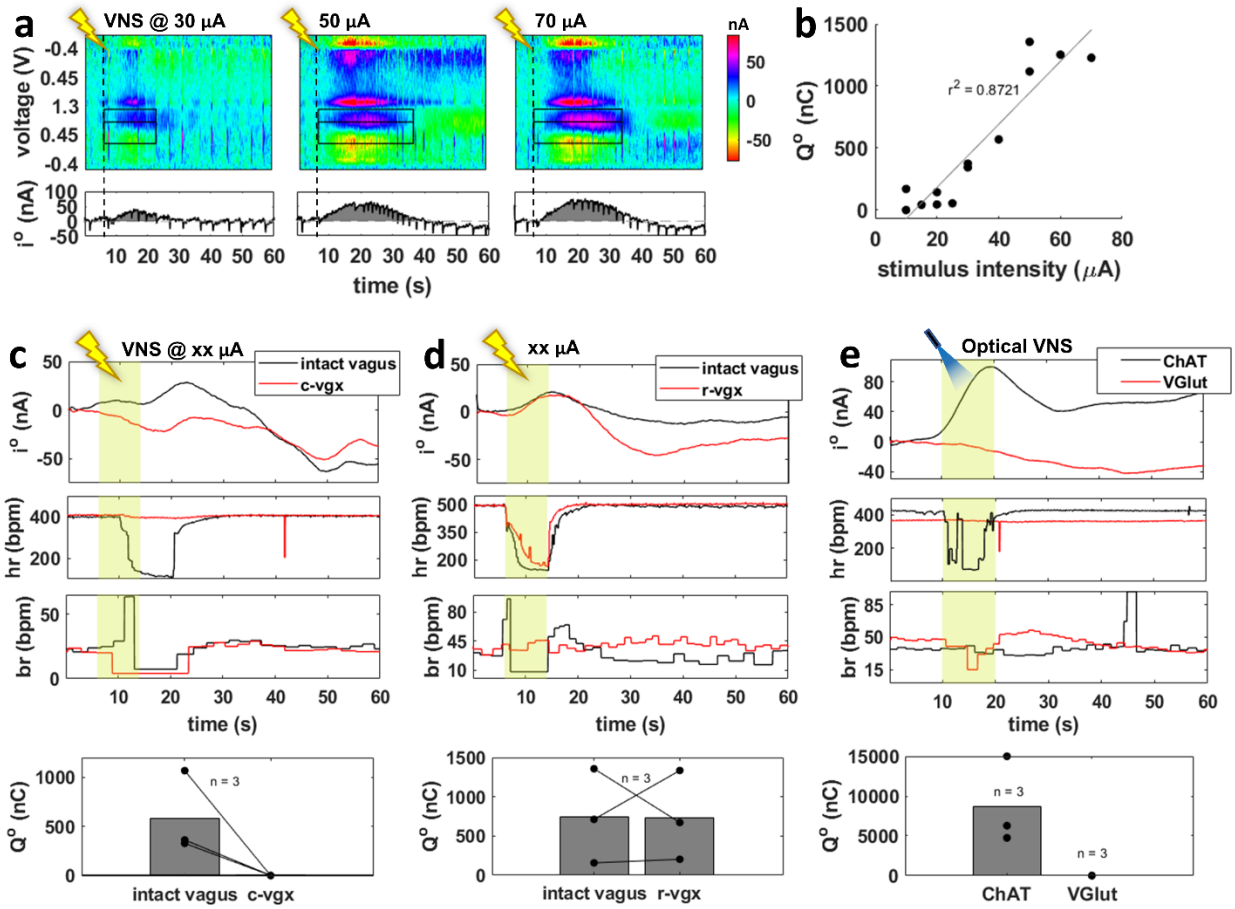

Figure 3. Stimulation of the efferent cervical vagus nerve elicits a NE signal in the spleen voltammogram. (a) Representative spleen voltammograms elicited by cervical vagus nerve stimulation (VNS). *Top and bottom panels* similar to those in Fig. 1d. The dashed vertical line denotes time of VNS. (b) NE oxidation charge in response to different VNS intensities (one representative of 3 animals). (c) NE oxidation current elicited by VNS (top panel), along with the associated heart rate and breathing rate responses (2 middle panels) and NE oxidation charge values (bottom panel), in animals with intact vagus and after caudal vagotomy (Vgx). (d) Same as (c), but for rostral vagotomy. (e) Representative NE current trace elicited by optogenetic stimulation of the vagus in ChAT-ChR or VGlut-ChR mice (top panel), along with the associated heart rate and breathing rate response (2 middle panels) and NE oxidation charge values (bottom panel).

Discussion

Bioelectronic medicine therapies deliver neurostimulation to autonomic nerves, aiming to modulate the function of specific organs that are affected by diseases. For improved efficacy and safety, clinical programming of bioelectronic therapies may use organ-specific biomarkers indicating target organ engagement and correlating with short- or long-term clinical responsiveness. Ideally, such biomarkers would be measurable in real-time, to allow personalized calibration of stimulation parameters. Our work suggests that voltammetry of the spleen can be such a real-time physiological biomarker for assessing NE release, in response to bioelectronic stimulation of the autonomic nervous system.

NE is the principal neurotransmitter of the sympathetic nervous system, a division of the peripheral ANS [17]. It belongs to a group of electrically active compounds termed catecholamines, which include epinephrine and dopamine [18]. Due to its redox properties, changes in NE can be detected by voltammetry at potentials unique to its chemical structure. FSCV can detect these changes immediately and at low concentrations owing to its high cycling speed of 400 V/s at 10 Hz and microscale working electrode [19]. When present in buffered saline, NE oxidizes at ~ 0.6 V and reduces at ~ –0.2 V using standard FSCV parameters. These values closely resemble what's recorded in FSCV brain studies looking at NE release dynamics [20]. However, when probing complex media such as the blood, one study found an increase in these redox potentials in vitro [21]. We recorded a similar increase in oxidation potentials at ~ 0.7 V in blood in vitro, which seemed to also increase with increasing NE concentration up to ~ 0.8 V. One possible explanation for this increase is biofouling of the voltammetry electrodes. Biofouling is a common issue that arises when electrochemical probes are implanted in biological tissues [22]. A layer of deposited biological material changes the electrodes' electrochemical impedance such that it requires higher voltage potentials to oxidize NE, which is consistent with what we and others have observed [21, 22]. This could be reduced by applying periods of high voltage and frequency cycling to re-new the surface of the electrode [21, 23]. Also, employing a three-electrode system might counteract fouling and prevent shifts in redox potentials [22]. Further, we found that the shape of the NE voltammogram in blood in vitro slightly differs than that reported in buffer, possibly due to shifts in background current over the period of scanning, which is consistent with reported observations [21].

These data provided an approximation of what to expect in peripheral tissues in vivo, especially in blood-filled organs such as the spleen. Measuring NE in vivo by probing the dynamic blood pool in the spleen—as NE is injected systemically—produced a similar voltammogram and increased oxidation potentials. We, however, noticed slight alterations in the signal profile compared to ex vivo blood. Typically, a background-subtracted voltammogram features current peaks that correspond to the oxidation and reduction of compounds in solution. In addition to a shift in baseline caused by background drift, we observed global changes in current at various potentials including the switching potential (1.3 V). Similar changes have been encountered, particularly at the reduction phase of the voltammogram, when measuring catecholamines at supraphysiologic concentrations [24], with the mechanism believed to be related to changes in the rate of dopamine adsorption to the electrode. Given the supraphysiologic concentrations of NE likely induced in this study (IV bolus injection, sp-stm, VNS) and the high estimated detection limit, this may be a reason for the observed reduction phase shift that we have observed throughout our experiments. Notably, the threshold of detection of injected NE was about 300nM, using a volume of distribution of 2 ml to estimate final blood concentration. This threshold is relatively high given that values of 30-60 nM are reported after some forms of neuromodulation [25, 26]. However, these reported values are determined in processed blood samples using ELISA or mass spectrometry where sample collection is typically delayed and therefore the true circulating values might be higher. Moreover, probing for NE close to the source nerve terminals might result in higher signals.

The spleen is a secondary lymphoid organ that continuously samples the blood offering a window into the circulation [27, 28]. It has emerged as a major target organ for bioelectronic therapies in the treatment of many inflammatory and chronic diseases. The spleen is innervated by a mesh-like network of adrenergic fibers that permeate the organ and lie in close proximity to immune cells [29, 30]. These fibers originate from post-ganglionic sympathetic neurons in the celiac ganglion with axons traveling to the spleen via the splenic nerve. The spleen has been identified as a critical component of the inflammatory reflex, a neural arc that senses inflammation in the periphery and responds with modulatory signals to the spleen via the vagus nerve [31-33]. The anti-inflammatory actions of splenic neuromodulation have been described using vagus nerve and splenic nerve stimulation as well as ultrasound insonification of the

spleen itself [2, 8, 34-36]. These therapeutic effects have been found to be mediated by NE released into the spleen from its intrinsic nerve fibers upon neuromodulation [3, 15]. In these studies, NE release was inferred using biochemical assays to measure NE in splenic homogenates or by recording splenic nerve activity. However, such techniques do not provide insight into NE release dynamics. Using FSCV, we recorded a NE signal elicited by electrical stimulation of the splenic neurovascular bundle almost immediately after delivery of the stimulus. The signal magnitude, which reflects amount of NE released, was dose-dependent on stimulation intensity, which is typical behavior of neural tissue. VNS has also been shown to modulate splenic function in a splenic nerve dependent manner [15]. Efferent vagal fibers are thought to relay signals to the splenic nerve via the celiac ganglion [33, 37]. Consistent with these reports, we recorded a NE signal in the spleen in real-time upon VNS. However, the signal was consistently of lower magnitude compared with splenic bundle stimulation even with maximal stimulation (determined by heart rate response). A possible explanation may be that VNS only relays to a subset of splenic nerve fibers, given that the putative vagal-splenic relay in the celiac ganglion is still structurally uncharacterized. This could imply that VNS at lower intensities might induce NE levels that fall below the limit of detection of this method with the current configuration. Studies that demonstrated VNS anti-inflammatory actions without inducing a reduction in heart rate support this notion [35]. The fact that the VNS-elicited signal correlated with heart rate reduction suggests that it might reflect sympathetic NE release into the circulation in response to a drop in blood pressure caused by VNS-induced change in heart rate [38]. This is supported by our observation that equivalent drops in heart rate induce by a beta-blocker produced a similar NE signal. The Ability to probe systemic changes in NE via the spleen might be useful in studying cardiovascular disease, expanding the utility of splenic probing. For example, changes in circulating NE could be used to titer and continually adjust a neuromodulation therapy aimed at treating hypotension. Notably, the signal magnitude varied across animals regardless of the stimulated nerve, possibly due to differences in electrode placement which will affect the number of fibers receiving stimulation. Additionally, the location of the voltammetry electrode in the spleen relative to nerve endings might influence the signal and is difficult to standardize given the lack of anatomical landmarks.

In order to provide precision therapies, the field of bioelectronic medicine must develop tools to monitor and adjust neuromodulation. FSCV in the spleen can detect NE in real-time offering a marker of ANS activity. Developing this approach to include multiple electrodes will enhance its sensitivity and reduce fouling when implanted chronically. Such systems could be used pre-clinically to resolve circuits and identify new targets for neuromodulation. Once optimized, voltammetry electrodes could be integrated in neuromodulation systems to continuously adjust therapeutic parameters and monitor response.

Acknowledgments

The authors thank Kip Ludwig and James Trevanthan from The Department of Biomedical Engineering, University of Wisconsin-Madison, and Shyue-An Chan and Corey Smith from the Department of Physiology and Biophysics, Case Western Reserve University for their helpful discussions.

References

1. Kenney MJ, Ganta CK. Autonomic nervous system and immune system interactions. Compr Physiol. 2014;4(3):1177-200.

2. Donega M, Fjordbakk CT, Kirk J, Sokal DM, Gupta I, Hunsberger GE, et al. Human-relevant near-organ neuromodulation of the immune system via the splenic nerve. Proc Natl Acad Sci U S A. 2021;118(20).

3. Rosas-Ballina M, Olofsson PS, Ochani M, Valdes-Ferrer SI, Levine YA, Reardon C, et al. Acetylcholine-synthesizing T cells relay neural signals in a vagus nerve circuit. Science. 2011;334(6052):98-101.

4. Birmingham K, Gradinaru V, Anikeeva P, Grill WM, Pikov V, McLaughlin B, et al. Bioelectronic medicines: a research roadmap. Nat Rev Drug Discov. 2014;13(6):399-400.

5. Koopman FA, Chavan SS, Miljko S, Grazio S, Sokolovic S, Schuurman PR, et al. Vagus nerve stimulation inhibits cytokine production and attenuates disease severity in rheumatoid arthritis. Proc Natl Acad Sci U S A. 2016;113(29):8284-9.

6. Kaniusas E, Kampusch S, Tittgemeyer M, Panetsos F, Gines RF, Papa M, et al. Current Directions in the Auricular Vagus Nerve Stimulation II - An Engineering Perspective. Front Neurosci. 2019;13:772.

7. Kaniusas E, Kampusch S, Tittgemeyer M, Panetsos F, Gines RF, Papa M, et al. Current Directions in the Auricular Vagus Nerve Stimulation I - A Physiological Perspective. Front Neurosci. 2019;13:854.

8. Zachs DP, Offutt SJ, Graham RS, Kim Y, Mueller J, Auger JL, et al. Noninvasive ultrasound stimulation of the spleen to treat inflammatory arthritis. Nat Commun. 2019;10(1):951.

9. Bonaz B, Sinniger V, Hoffmann D, Clarencon D, Mathieu N, Dantzer C, et al. Chronic vagus nerve stimulation in Crohn's disease: a 6-month follow-up pilot study. Neurogastroenterol Motil. 2016;28(6):948-53.

10. Ben-Menachem E. Vagus nerve stimulation, side effects, and long-term safety. J Clin Neurophysiol. 2001;18(5):415-8.

11. Mulders DM, de Vos CC, Vosman I, van Putten MJ. The effect of vagus nerve stimulation on cardiorespiratory parameters during rest and exercise. Seizure. 2015;33:24-8.

12. Chang YC, Cracchiolo M, Ahmed U, Mughrabi I, Gabalski A, Daytz A, et al. Quantitative estimation of nerve fiber engagement by vagus nerve stimulation using physiological markers. Brain Stimul. 2020;13(6):1617-30.

13. Goyal RK, Chaudhury A. Physiology of normal esophageal motility. J Clin Gastroenterol. 2008;42(5):610-9.

14. Harkness J, Wagner J. Biology and husbandry. The biology and medicine of rabbits and rodents. 1989:372.

15. Rosas-Ballina M, Ochani M, Parrish WR, Ochani K, Harris YT, Huston JM, et al. Splenic nerve is required for cholinergic antiinflammatory pathway control of TNF in endotoxemia. Proc Natl Acad Sci U S A. 2008;105(31):11008-13.

16. Ahmed U, Chang YC, Cracchiolo M, Lopez MF, Tomaio JN, Datta-Chaudhuri T, et al. Anodal block permits directional vagus nerve stimulation. Sci Rep. 2020;10(1):9221.

17. Karemaker JM. An introduction into autonomic nervous function. Physiological Measurement. 2017;38(5):R89-R118.

18. Molinoff PB, Axelrod J. Biochemistry of catecholamines. Annu Rev Biochem. 1971;40:465-500.

19. Rodeberg NT, Sandberg SG, Johnson JA, Phillips PE, Wightman RM. Hitchhiker's Guide to Voltammetry: Acute and Chronic Electrodes for in Vivo Fast-Scan Cyclic Voltammetry. ACS Chem Neurosci. 2017;8(2):221-34.

20. Park J, Takmakov P, Wightman RM. In vivo comparison of norepinephrine and dopamine release in rat brain by simultaneous measurements with fast-scan cyclic voltammetry. J Neurochem. 2011;119(5):932-44.

21. Nicolai EN, Trevathan JK, Ross EK, Lujan JL, Blaha CD, Bennet KE, et al. Detection of Norepinephrine in Whole Blood via Fast Scan Cyclic Voltammetry. IEEE Int Symp Med Meas Appl. 2017;2017:111-6.

22. Seaton BT, Hill DF, Cowen SL, Heien ML. Mitigating the Effects of Electrode Biofouling-Induced Impedance for Improved Long-Term Electrochemical Measurements In Vivo. Anal Chem. 2020;92(9):6334-40.

23. Takmakov P, Zachek MK, Keithley RB, Walsh PL, Donley C, McCarty GS, et al. Carbon microelectrodes with a renewable surface. Anal Chem. 2010;82(5):2020-8.

24. Johnson JA, Hobbs CN, Wightman RM. Removal of Differential Capacitive Interferences in Fast-Scan Cyclic Voltammetry. Anal Chem. 2017;89(11):6166-74.

25. Liu S, Wang Z, Su Y, Qi L, Yang W, Fu M, et al. A neuroanatomical basis for electroacupuncture to drive the vagal-adrenal axis. Nature. 2021;598(7882):641-5.

26. Torres-Rosas R, Yehia G, Pena G, Mishra P, del Rocio Thompson-Bonilla M, Moreno-Eutimio MA, et al. Dopamine mediates vagal modulation of the immune system by electroacupuncture. Nat Med. 2014;20(3):291-5.

27. Lewis SM, Williams A, Eisenbarth SC. Structure and function of the immune system in the spleen. Sci Immunol. 2019;4(33).

28. Mebius RE, Kraal G. Structure and function of the spleen. Nat Rev Immunol. 2005;5(8):606-16.

29. Ding X, Wang H, Qian X, Han X, Yang L, Cao Y, et al. Panicle-Shaped Sympathetic Architecture in the Spleen Parenchyma Modulates Antibacterial Innate Immunity. Cell Rep. 2019;27(13):3799-807 e3.

30. Hu D, Al-Shalan HAM, Shi Z, Wang P, Wu Y, Nicholls PK, et al. Distribution of nerve fibers and nerve-immune cell association in mouse spleen revealed by immunofluorescent staining. Sci Rep. 2020;10(1):9850.

31. Pavlov VA, Tracey KJ. The cholinergic anti-inflammatory pathway. Brain Behav Immun. 2005;19(6):493-9.

32. Tracey KJ. Reflex control of immunity. Nat Rev Immunol. 2009;9(6):418-28.

33. Pavlov VA, Chavan SS, Tracey KJ. Molecular and Functional Neuroscience in Immunity. Annu Rev Immunol. 2018;36:783-812.

34. Borovikova LV, Ivanova S, Zhang M, Yang H, Botchkina GI, Watkins LR, et al. Vagus nerve stimulation attenuates the systemic inflammatory response to endotoxin. Nature. 2000;405(6785):458-62.

35. Huffman WJ, Subramaniyan S, Rodriguiz RM, Wetsel WC, Grill WM, Terrando N. Modulation of neuroinflammation and memory dysfunction using percutaneous vagus nerve stimulation in mice. Brain Stimul. 2019;12(1):19-29.

36. Mughrabi IT, Hickman J, Jayaprakash N, Thompson D, Ahmed U, Papadoyannis ES, et al. Development and characterization of a chronic implant mouse model for vagus nerve stimulation. Elife. 2021;10.

37. Kressel AM, Tsaava T, Levine YA, Chang EH, Addorisio ME, Chang Q, et al. Identification of a brainstem locus that inhibits tumor necrosis factor. Proc Natl Acad Sci U S A. 2020;117(47):29803-10.

38. Grossman SH, Davis D, Gunnells JC, Shand DG. Plasma norepinephrine in the evaluation of baroreceptor function in humans. Hypertension. 1982;4(4):566-71.